Developmental Biology 364 (2012) 149–161

Contents lists available at SciVerse ScienceDirect

Developmental Biology

journal homepage: www.elsevier.com/developmentalbiology

Sostdc1 defines the size and number of skin appendage placodes

Katja Närhi [a], Mark Tummers [a], Laura Ahtiainen [a], Nobuyuki Itoh [b], Irma Thesleff [a], Marja L. Mikkola [a,*]

[a] Developmental Biology Program, Institute of Biotechnology, University of Helsinki, P.O. Box 56, 00014 Helsinki, Finland
[b] Department of Genetic Biochemistry, Kyoto University Graduate School of Pharmaceutical Sciences, Kyoto 606-8501, Japan

ARTICLE INFO

Article history:
Received for publication 30 November 2011
Revised 29 January 2012
Accepted 30 January 2012
Available online 8 February 2012

Keywords:
Vibrissa
Mammary gland
Hair
Wise
Ectodin
Usag-1

ABSTRACT

Mammary glands and hair follicles develop as ectodermal organs sharing common features during embryonic morphogenesis. The molecular signals controlling the initiation and patterning of skin appendages involve the bone morphogenetic proteins and Wnt family members, which are commonly thought to serve as inhibitory and activating cues, respectively. Here, we have examined the role of the Bmp and Wnt pathway modulator Sostdc1 in mammary gland, and hair and vibrissa follicle development using *Sostdc1*-null mice. Contrary to previous speculations, loss of Sostdc1 did not affect pelage hair cycling. Instead, we found that Sostdc1 limits the number of developing vibrissae and other muzzle hair follicles, and the size of primary hair placodes. Sostdc1 controls also the size and shape of mammary buds. Furthermore, Sostdc1 is essential for suppression of hair follicle fate in the normally hairless nipple epidermis, but its loss also promotes the appearance of supernumerary nipple-like protrusions. Our data suggest that functions of Sostdc1 can be largely attributed to its ability to attenuate Wnt/β-catenin signaling.

Introduction

The development of skin appendages such as the hair follicle, feather, mammary gland, and tooth shares a great number of morphological and molecular commonalities (Mikkola, 2007; Mikkola and Millar, 2006). All these organs are initiated as placodes, local thickenings of the epithelium, which invaginate the mesenchyme to form a bud. In each organ, these early steps of morphogenesis depend on a few essential signaling pathways the Wnt/β-catenin and TGFβ, in particular Bmp, pathways being amongst the most important ones. While the formation of hair and mammary placodes is absolutely dependent on epithelial Wnt/β-catenin activity (Andl et al., 2002; Chu et al., 2004; Zhang et al., 2009), the role of Bmp signaling in placode formation is more elusive. Bmps, in particular Bmp4, are generally considered as inhibitors of hair placode formation. Excess Bmp4 inhibits hair and feather placode formation in vitro (Jung et al., 1998; Noramly and Morgan, 1998; Pummila et al., 2007). Deficiency in noggin, a potent Bmp inhibitor, leads to severely reduced number of hair placodes (Botchkarev et al., 1999), while its overexpression results in increased hair density (Plikus et al., 2004). On the other hand, Bmp7 has been proposed to support feather placode formation (Harris et al., 2004; Michon et al., 2008). Function of the Bmp pathway in mammary placode formation is poorly understood.

It is evident that for proper patterning and morphogenesis of ectodermal organs, the activity of these two key signaling pathways needs to be tightly controlled both in space and time (Lin et al., 2006; Mikkola and Millar, 2006; Schneider et al., 2009; Tummers and Thesleff, 2009). In general, the expression of the Wnt and Bmp ligands is more restricted while their receptors are more broadly distributed. An additional level of regulation is achieved through a number of extracellular modulators, which also typically show a dynamic and focal expression pattern. In hair placodes, Wnt antagonists Dickkopf-1 and -4 (Dkk1 and Dkk4) are expressed in the condensed mesenchyme and the epithelial placode, respectively, and Dkk4 is also expressed in mammary and tooth placodes (Andl et al., 2002; Bazzi et al., 2007; Fliniaux et al., 2008). In addition, certain soluble Frizzled-related proteins (sFRPs), as well as Wif1, are expressed in developing skin appendages (Kiyozumi et al., 2010; Leimeister et al., 1998). However, despite the apparent importance of Wnt inhibitors in hair placode patterning (Andl et al., 2002; Sick et al., 2006) loss-of-function studies have not revealed the involvement of any particular Wnt inhibitor in hair follicle spacing, possibly owing to functional redundancy. Of the TGFβ pathway modulators implicated in hair follicle pattering including noggin, ctgf (Ccn2), and follistatin (Mou et al., 2006; Pummila et al., 2007), only noggin is known to affect hair placode formation in vivo (Botchkarev et al., 1999; Plikus et al., 2004).

Accumulating evidence indicates that Sostdc1, a protein related to the bone density regulator Sclerostin (Laurikkala et al., 2003), can regulate both Wnt and Bmp pathways. Sostdc1 is a highly conserved, vertebrate-specific secreted protein that was independently isolated and named three times as Usag-1 in rat (Simmons and Kennedy, 2002), ectodin in mouse (Laurikkala et al., 2003), and Wise in chicken (Itasaki et al., 2003). Sostdc1 has a clear antagonistic effect on Bmp signaling, apparently through its ability to directly bind to Bmp2, -4,

* Corresponding author. Fax: +358 9 19159366.
E-mail address: marja.mikkola@helsinki.fi (M.L. Mikkola).

0012-1606/$ – see front matter © 2012 Elsevier Inc. All rights reserved.
doi:10.1016/j.ydbio.2012.01.026

-6, and -7 (Laurikkala et al., 2003; Yanagita et al., 2004). In vitro, Sostdc1 inhibits the ability of Bmps to promote osteoblast differentiation in a dose-dependent manner (Laurikkala et al., 2003; Yanagita et al., 2004). Sostdc1 has also been shown to suppress Bmp7-induced phosphorylation of R-Smads-1, -5, and -8 in kidney cancer cell lines (Blish et al., 2008). In cultured embryonic tooth explants recombinant Sostdc1 can prevent Bmp2 and Bmp7-induced expression of the Bmp target gene *Msx2* (Laurikkala et al., 2003), and *Sostdc1* deficiency sensitizes cultured tooth buds to excess Bmp (Kassai et al., 2005).

The function of Sostdc1 as a Wnt pathway modulator appears more complex. Data obtained in *Xenopus* suggest that Sostdc1 has a dual role such that it can either suppress or promote canonical Wnt activity in a context dependent manner (Itasaki et al., 2003). However, in mammalian systems Sostdc1 has thus far only been shown to act as a Wnt antagonist and was shown to block Wnt1, Wnt3a, and Wnt10b activities in reporter assays in cultured cells (Beaudoin et al., 2005; Blish et al., 2008; Yanagita et al., 2004). The ability of Sostdc1 to inhibit Wnt/β-catenin signaling has been attributed to its capability to compete with Wnt ligands for binding to Lrp6, the Wnt co-receptor involved in canonical Wnt signaling (Ahn et al., 2010; Itasaki et al., 2003; Lintern et al., 2009).

Sostdc1 is expressed in many developing skin appendages including teeth, taste papillae, and hair and vibrissa follicles (Ahn et al., 2010; Kassai et al., 2005; Laurikkala et al., 2003; Närhi et al., 2008; O'Shaughnessy et al., 2004). So far, the function of Sostdc1 has been analyzed in developing teeth only where it is essential for proper cusp patterning of molar teeth (Ahn et al., 2010; Kassai et al., 2005). In addition, its loss leads to formation of supernumerary incisors and premolar-like teeth (Kassai et al., 2005; Munne et al., 2009; Murashima-Suginami et al., 2007). Interestingly, studies on *Hairless* (*Hr*) mutant mice suggested involvement of Sostdc1 in hair follicle cycling (Beaudoin et al., 2005). Here we have analyzed the consequences of *Sostdc1* deficiency in hair and mammary gland development. We show that Sostdc1 is dispensable for hair follicle cycling but it regulates the number, size and/or shape of vibrissa, hair and mammary buds.

Materials and methods

Animals and preparation of embryonic tissues

The generation and genotyping of *Sostdc1*-null mice have been described previously (Kassai et al., 2005). RT-PCR and in situ hybridization analysis confirmed absence of *Sostdc1* transcripts in developing mammary buds and hair follicles (data not shown). *Sostdc1*-mutant mice were maintained in C57Bl/6 background. Despite the inserted LacZ-construct in the *Sostdc1* locus, the overnight X-gal staining of *Sostdc1*+/− or *Sostdc1*−/− embryos resulted in only very weak β-galactosidase activity in developing skin appendages (data not shown) allowing us to use TOP-gal (DasGupta and Fuchs, 1999) and BAT-gal (Maretto et al., 2003) mice for analysis of the Wnt pathway activity. K17-GFP mice (Bianchi et al., 2005) were used to visualize developing skin appendages. All aspects of mouse care and experimental protocols were approved by the National Board of Animal Experimentation.

To obtain staged embryos, the appearance of a vaginal plug was taken as embryonic day (E) 0, and embryos were further staged according to morphological criteria. Whole embryos or dissected tissues were fixed in 4% paraformaldehyde (PFA) and taken through ethanol series and xylene into paraffin, and serially sectioned at 7 μm for histology, in situ hybridization, and immunohistochemistry. Adult nipples were dissected from pregnant mice. Sections for normal histology were stained with hematoxylin and eosin, or nuclear fast red. Hair cycle analysis was according to Muller-Rover et al. (2001). Pictures of sections were taken with Olympus Provis microscope.

In situ hybridization and immunohistochemistry

Whole-mount and radioactive in situ hybridization was performed as previously described (Närhi et al., 2008). The following probes were used: *Sostdc1* (Laurikkala et al., 2003), *Wnt10b* (Wang and Shackleford, 1996), *β-catenin*, *Lef1* (Laurikkala et al., 2002), and *Id1* (Rice et al., 2000). To detect keratin2e, keratin82, or Lef1, deparaffinized and citrate-treated sections were stained with the Vectastain Elite ABC Kit (Vector). Samples were blocked with 5% goat serum–3% BSA in PBS (for keratin2e) or 5% goat serum in TBS-0.1% Tween (for Lef1 and keratin82), and anti-keratin2e antibody (1: 200, Fitzgerald), anti-keratin82 (1:300, Abgent), or anti-Lef1 (1:1000, Cell Signaling Technology) was used with the appropriate secondary antibody (Vector). Detection of Ki67 was performed on serial paraffin sections with anti-Ki67 antibody (1:500; Neomarkers) and with UltraVision Detection System kit (Thermo Scientific). In cell proliferation assays, mice were injected with 1 ml/100 g body weight of 5′-bromo-2′-deoxyuridine (BrdU) labeling reagent (Amersham) 2 h before sacrifice, and BrdU was detected in serial paraffin sections after unmasking with trypsin using anti-BrdU-antibody (Ab-3, Thermo Scientific, 1:1000) and M.O.M. peroxidase kit (Vector). For whole-mount EpCAM immunofluorescence staining, ventral tissue encompassing mammary buds 2–4 was dissected. Methanol-fixed samples were blocked with 5% donkey serum and 0.5% BSA in 0.1% Triton X-100-PBS (PBST) and anti-EpCAM-antibody (1:1000, BD Pharmingen) was used with 488 AlexaFluor secondary antibody (Invitrogen) followed by several washes with PBST and post-fixation by 4% PFA before mounting (Vectashield). The images were documented with Leica SP5 laser scanning confocal microscope and bud volume was measured with Imaris 7.2.1 software (Bitplane).

Oil-Red-O staining

Adult skin pieces with mammary glands and nipples were fixed in 4% PFA for 24 h and then processed to 10 μm cryosections. Air-dried cryosections were further fixed in ice-cold 10% formalin for 10 min and rinsed with distilled water. Dry samples were incubated in 100% propylene glycol for 5 min (Sigma) before 10-minute Oil Red O-staining (Sigma) at room temperature. Samples were rinsed twice with 85% propylene glycol and distilled water before counterstaining with hematoxylin and mounting.

X-gal staining

TOP-gal or BAT-gal embryos were stained with X-gal staining solution for 1, 3, or 24 h as described (Järvinen et al., 2006).

Statistical comparison

All statistical comparisons were carried out between mutants and their littermate controls. Cell^{A} software (Soft Imaging System GmbH) was used to measure the distance between mammary buds using E13.0–E13.5 whole-mounts showing K17-GFP, TOP-gal, or placodal marker gene expression. Quantification of cells expressing placode markers between buds 1 and 2, 2 and 3, or 4 and 5 was done on E13.0–13.5 specimen whole-mount stained for TOP-gal, or placodal markers. The size of primary hair placodes was measured from K17-GFP and *Wnt10b* whole-mount samples with Image-Pro Plus 5.1. Wilcoxon signed ranks test was used for statistical analysis except for comparison of bud volume which was done with student's t-test. Number of specimens analyzed is indicated in figure legends.

3D reconstruction

Pictures of transversally cut serial sections (7 μm) of E13.5 TOP-gal-mammary buds were reconstructed for 3D by the Scion Image software (version 4) as described (Järvinen et al., 2009).

Tissue culture

E13 skin covering lower mandible and the vibrissa pad of E13 K17-GFP;*Sostdc1*−/− and K17-GFP;*Sostdc1*+/+ embryos were dissected in Dulbecco's PBS (pH 7.4) under a stereomicroscope. Explants were cultured for three days in a Trowell type culture as described (Närhi and Thesleff, 2010). The vibrissa explants were photographed with Leica MZFLIII fluorescent stereomicroscope.

Mammary gland whole mounts

Embryonic and postnatal fat pads containing mammary glands of virgin and pregnant *Sostdc1*-deficient and control littermates were dissected and spread on a glass slide to air dry for 30 min. The following steps were all performed at room temperature. After 2–4 hour fixation in Carnoy's fixative (6:1 100% EtOH:glacial acetic acid) sample slides were gradually processed to distilled water starting with 70% EtOH. Samples were stained in carmine alum (carmine, Sigma; aluminum potassium sulfate, Sigma) for 24 h, dehydrated through EtOH series to xylene, and mounted. Specimens were photographed with a stereomicroscope (Olympus SZX9).

Results

Patterns of Sosdc1 expression during early appendage development

In order to get insights into the role of Sostdc1 in developing hair and mammary glands, we first analyzed its embryonic expression pattern (Fig. 1). Strong *Sostdc1* expression was detected in the vibrissa pad, even prior to placode formation (Fig. 1A; data not shown), and later *Sostdc1* was expressed in a ring-like pattern around both sensory and mystacial vibrissa buds (Fig. 1C). Vibratome sections and radioactive in situ hybridization confirmed that *Sostdc1* transcripts were confined to the epithelium (Fig. 1C, D). *Sostdc1* expression appeared early

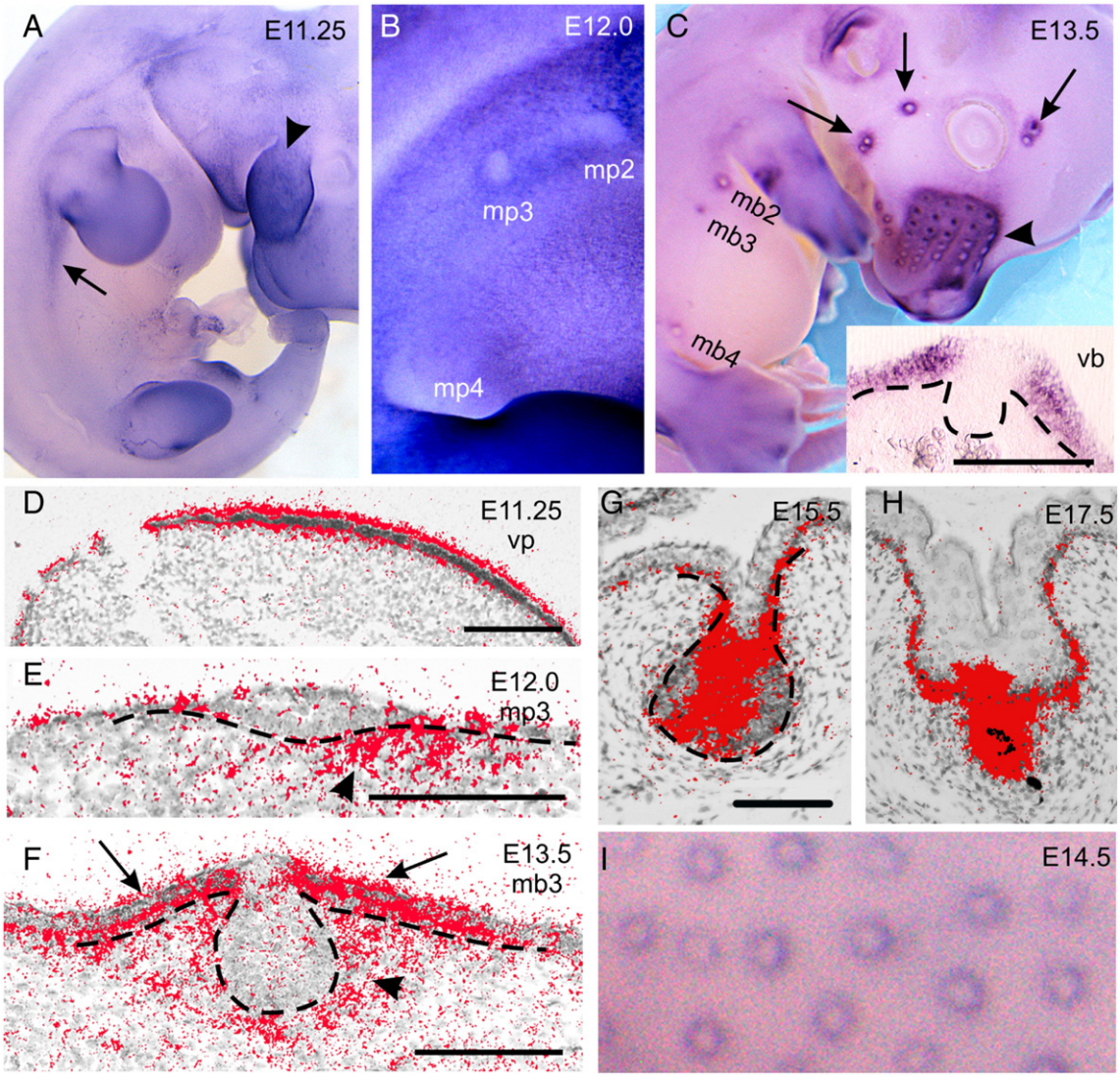

Fig. 1. *Sostdc1* expression pattern in developing mammary glands, vibrissae, and primary hair placodes. (A–C, I) Whole-mount and (D–H) radioactive in situ hybridization with a probe specific to *Sostdc1*. (A) At E11.25, *Sostdc1* showed expression in early mammary region (arrow) and in the ectoderm of developing vibrissae pad (vp; arrowhead). (B) At E12.0, *Sostdc1* expression was downregulated in mammary placodes (mp). (C) At E13.5, strong expression was detected in the whisker pad (arrowhead) and around the mammary (mb), mystacial vibrissae (arrowhead), and facial sensory hair buds (arrows). Insert shows vibratome section of a vibrissae bud (vb). Expression of *Sostdc1* in the vibrissae pad epithelium at E11.25 (D). In developing mammary glands transcripts were detected in the mesenchyme and epithelium at E12.0 (E), but at E13.5 (F), E15.5 (G), and at E17.5 (H) expression was largely confined to the epithelium. (I) *Sostdc1* surrounded the E14.5 hair placodes. Scale bars 100 μm.

also in the mammary gland region (Fig. 1A). When mammary placodes were emerging, *Sostdc1* expression was high around the placodes, and transcripts were detected both in the mesenchyme and the epithelium (Fig. 1B, E). At the bud stage, vibratome sections verified that high epithelial *Sostdc1* expression surrounded the mammary buds (data not shown), but the more sensitive radioactive in situ hybridization technique revealed some transcripts also in the mesenchyme (Fig. 1C, F). Later, *Sostdc1* was observed throughout the mammary epithelium (Fig. 1G). Prominent expression was detected in the primary mammary sprout, as well as in epithelial cells facing the basement membrane (Fig. 1H). In hair follicles, *Sostdc1* expression marked the edges of nascent hair placodes (Fig. 1I; Laurikkala et al., 2003). Expression of *Sostdc1* is induced by Bmps in embryonic tooth (Laurikkala et al., 2003) and E14 skin epithelial explants (Mou et al., 2006). Several Bmps are expressed in hair follicle primordia, but Bmp inhibitors expressed in the placode (or the underlying dermal condensate) are thought to block Bmp signaling in placodal cells (Botchkarev et al., 1999; Mou et al., 2006; Pummila et al., 2007) thereby limiting Bmp activity to the surroundings. This likely explains the ring-like expression pattern of *Sostdc1*. Whether Bmps regulate *Sostdc1* expression also in mammary buds is currently not known.

Enlarged mammary buds of Sostdc1 embryos are associated with ectopic Wnt activity

In mouse, five pairs of mammary placodes form in a characteristic order and position along the flanks of the embryos (Veltmaat et al., 2003). Within 36 h a short line of multilayered epithelial cells progressively changes through a comet- and disc-shape into a bud, which is morphologically distinct from the surrounding epidermis. To address the role of Sostdc1 in developing mammary buds, we compared *Sostdc1*-null mice (Kassai et al., 2005) with their control littermates at E11.5 to E14.0. Mammary glands were visualized with *Lef1*, one of the earliest markers of developing mammary buds (Veltmaat et al., 2003). At E11.5, only mammary placode 3 was readily observed, and no difference was seen between *Sostdc1*-null and control embryos (Fig. 2A). By E12.0 well-defined mammary buds were visible in control embryos and *Lef1*-positive cells were detected between buds 1 and 2, and 2 and 3 in both control and mutant specimens (Fig. 2B). However, the *Lef1*-positive bud area was enlarged in *Sostdc1*-deficient embryos (Fig. 2B), an abnormality that became more evident by E13.5 (Fig. 2C). Moreover, *Lef1* expressing cells were still observed along the mammary line in mutant embryos at E13.5, between buds 1 and 2, 2 and 3, and 4 and 5 (Fig. 2C; data not shown). Similar findings were observed with two other markers *Wnt10b* and *β-catenin* (Fig. 2D, E, G; data not shown). Curiously, mammary buds 2 and 3 and occasionally buds 4 and 5 were located closer to each other in mutant embryos (Fig. 2B–F; see also Figs. 3D and 4C).

Analysis of hematoxylin–eosin stained serial transverse sections revealed that the width of the *Sostdc1*-null bud, especially in the neck area, was enlarged, and the mutant buds did not display the typical light bulb shape of control specimen, an abnormality that persisted until E14.0 (Fig. 3A, B and data not shown). 3D reconstructions of serial sections confirmed the large size and abnormal shape of *Sostdc1*-null mammary buds (Fig. 3C). Statistical analysis of confocal images of EpCAM stained whole-mounts (Fig. 3D) of *Sostdc1*−/− mammary buds 2 and 3 ($n_{mut}=4$; $n_{ctrl}=6$) verified the 3D reconstruction data: bud shape was altered and the volume of buds 2 ($volume_{ctrl}=3.8*10^5\,\mu m^3\pm 5.2*10^4\,\mu m^3$ (s.d.); $volume_{mut}=4.9*10^5\,\mu m^3\pm 6.6*10^4\,\mu m^3$; $P<0.05$) and 3 ($volume_{ctrl}=4.7*10^5\,\mu m^3\pm 4.8*10^4\,\mu m^3$; $volume_{mut}=6.5*10^5\pm 6.6*10^4$; $P<0.01$) was increased by 1.3-fold and 1.4-fold, respectively. Analysis of BrdU incorporation at E12.25 and E13.5 (Fig. 3E; Fig. S1A, B) or the number of Ki67-positive cells at E13.5 (Fig. 3F; Fig. S1C) did not reveal any difference between *Sostdc1*-null and control embryos suggesting that the increase in bud size is likely not due to enhanced cell proliferation.

To address the molecular mechanisms responsible for generating the observed mammary bud phenotype, we crossed *Sostdc1*-null mice with TOP-gal mice in which LacZ reporter is expressed at sites of canonical Wnt activity (DasGupta and Fuchs, 1999). Previous studies have revealed strong epithelial TOP-gal expression in mammary bud epithelium from E10.5 to E15.5 (Chu et al., 2004). While TOP-gal activity was detected along the mammary line and in forming buds both in control and *Sostdc1*-null embryos at E12.0, the number of TOP-gal positive cells was higher between buds 3 and 4 in mutant embryos (Fig. 4A). At E12.75 to E13.5 we did not detect gross difference in the intensity of TOP-gal expression between control and *Sostdc1*-null mammary buds either in whole mounts or in serial sections (Figs. 4B–D and S2; and data not shown). However, ectopic expression was evident along the milk line between neighboring buds (Fig. 4B, C; and data not shown), and in epithelial cells in the vicinity of the mammary bud (Fig. 4D; Fig. S2), and in the neck region at E15.5 (Fig. 4E), i.e. at sites of high *Sostdc1* expression (Fig. 1). Similar observations were made with the BAT-gal reporter (data not shown). 3D reconstructions of TOP-gal expressing mammary buds verified our findings (Fig. S2). Accordingly, strong ectopic expression of Lef1 protein was readily detected at E12.5 and E13.5 in epithelial cells next to the buds (Fig. 4F, G; Fig. S3A, B).

Effects of *Sostdc1* deficiency on BMP pathway activity were examined by analyzing expression levels of BMP target gene *Id1* (Hollnagel et al., 1999; Rice et al., 2000) and phosphoSMAD (pSMAD) 1/5/8 staining (Fig. S3). *Id1* was readily detected in the mammary mesenchyme (Fig. S3C) and pSMAD1/5/8 was observed both in mesenchymal and epithelial cells at E13.0 (Fig. S3D), but no differences were detected in expression intensities, or the number of pSMAD1/5/8-positive cells between control and *Sostdc1*-null mammary buds (Fig. S3D, E).

Ectopic nipple-like tissue forms in Sostdc1-null mice postnatally

Previous studies have shown that stimulation of Wnt/β-catenin activity in developing mammary glands, achieved through transgenic expression of Wnt1, Wnt10b, or Lrp6, accelerates ductal development and branching (Lane and Leder, 1997; Tsukamoto et al., 1988; Zhang et al., 2010), while deficiency in Lrp6 severely compromises epithelial growth and branching morphogenesis (Lindvall et al., 2009). Interestingly, the primary mammary sprout showed prominent *Sostdc1* expression. These findings prompted us to analyze *Sostdc1*-null mammary phenotype at later developmental stages. At E18, at the onset of puberty (P22), or at four weeks of age, no difference in ductal outgrowth or branching was observed between *Sostdc1*-null and control littermates (Fig. S4A–C, and data not shown). *Sostdc1*-null mammary epithelium responded normally to pregnancy-associated hormones, as well (Fig. S4D–E), and mutant females had no obvious difficulty in nursing their pups. Surprisingly, macroscopic examination of *Sostdc1*-null adult females revealed ectopic nipple-like structures in the vicinity of mammary gland 2 and 3 (Fig. 5A–D) in all mice analyzed ($n=12$), and also often next to all other glands (Fig. 5L; Fig. S5; data not shown). Supernumerary nipples were mostly located laterally to endogenous nipples, in their immediate proximity. In addition, endogenous nipples were wider (Fig. 5A–D). Strangely, the ectopic nipples were never macroscopically observed before puberty but became apparent around six weeks of age as the females approached maturity. Next we performed in situ hybridization in nipple sections of juvenile (3 and 4.5 week old) and adult pregnant mice. At all stages, we detected *Sostdc1* expression at high levels in basal cells of the main duct, but not elsewhere in the nipple epithelium or in the neighboring epidermis (Fig. S6; and data not shown). These results suggest that Sostdc1 plays a suppressive role in establishment rather than maintenance of nipple epithelial fate.

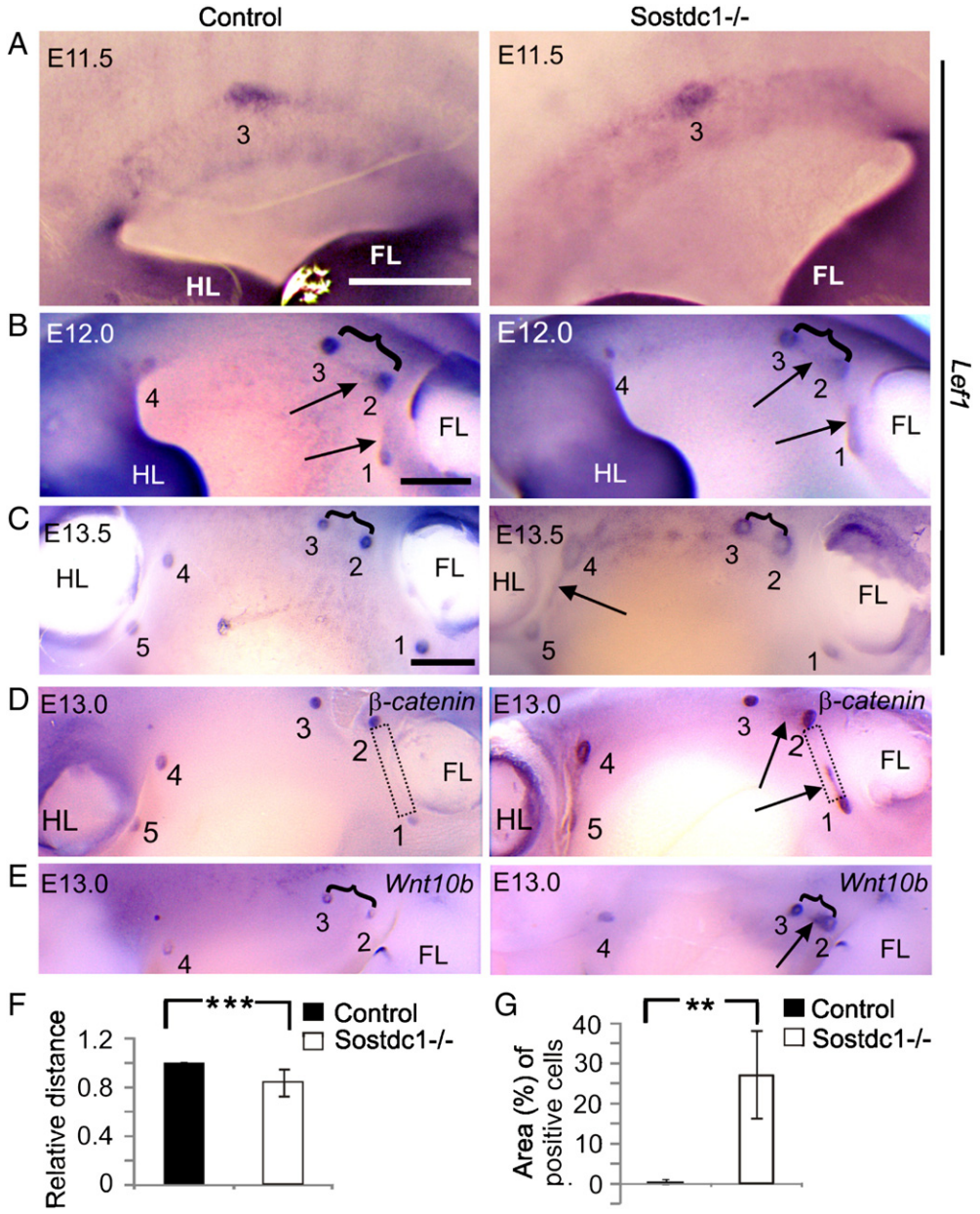

Fig. 2. *Sostdc1* deficiency resulted in enlarged mammary buds. (A–E) Expression patterns of *Lef1*, *β-catenin*, and *Wnt10b* during mammary bud formation by whole-mount in situ hybridization in control and *Sostdc1*−/− mice. Numbers denote the positions of the developing mammary glands. (A) At E11.5, no difference was detected in *Lef1* expression between control and mutant mammary placode 3 ($n_{ctrl}=6$, $n_{mut}=8$). At E12.0 (B; $n_{ctrl}=4$, $n_{mut}=3$) and E13.5 (C; $n=8$), an enlarged domain of *Lef1* expression was seen in *Sostdc1*−/− mammary buds compared to control mice. Brackets indicate shorter distance between *Sostdc1*−/− buds 2 and 3, compared to control mammary buds. *β-catenin* (D; $n_{ctrl}=5$, $n_{mut}=7$) and *Wnt10b* (E; $n_{ctrl}=7$, $n_{mut}=6$) also showed enlarged expression area in *Sostdc1*−/− mammary buds compared to control mice at E13.0. Arrows (B, C, E) point to *Lef1*-, *Wnt10b*- and *β-catenin*-positive cells between neighboring mammary buds. (F) Mean relative distance between buds 2 and 3 ± s.d. ($n=17$). (G) Mean area (% ± s.d) of cells positive for placode markers between neighboring buds ($n=19$). Dotted rectangle (E) indicates the region that was used to measure the area of positive cells. Scale bars 500 μm (A–E). FL, forelimb; HL, hindlimb. **P<0.01, ***P<0.001.

Unexpectedly, hair filaments often emerged from the normally hairless nipple area in *Sostdc1* mutants (see below). Serial sectioning revealed that aberrant pilosebaceous units were often embedded in endogenous (Fig. 5E–J; Fig. S5) and ectopic (Fig. 5K–M; Fig. S5C, D) nipples in the mutant mice, but never in the controls (Fig. 5; Fig. S5, and data not shown). Presence of sebaceous glands was confirmed by Oil-Red-O staining (Fig. 5G, H). Staining with antibody against keratin 2e, a specific marker for nipple epithelium (Mahler et al., 2004), verified that the ectopic nipple-like structures indeed had nipple identity (Fig. 5I, J, L). However, we never detected a ductal network associated with the supernumerary nipples (Fig. S4A–C; data not shown). Instead, a large hair follicle was located in the middle. The follicle stained positive for keratin82, a type II hair keratin, indicating proper hair formation, and frequently a hair filament protruded from the center of the nipples (Fig. 5K–M; Fig. S5C, D; data not shown). Despite the presence of aberrant follicle-like structures in endogenous nipples, no hair shafts were observed suggesting that these pilosebaceous units were not fully differentiated (data not shown).

Sostdc1-null mice have ectopic vibrissae

The strong expression of *Sostdc1* in the vibrissa pad (Fig. 1) prompted us to study the function of Sostdc1 in developing vibrissae. In mouse, primary (mystacial) vibrissa development shows a high degree of order and pattern (Davidson and Hardy, 1952; Wrenn and

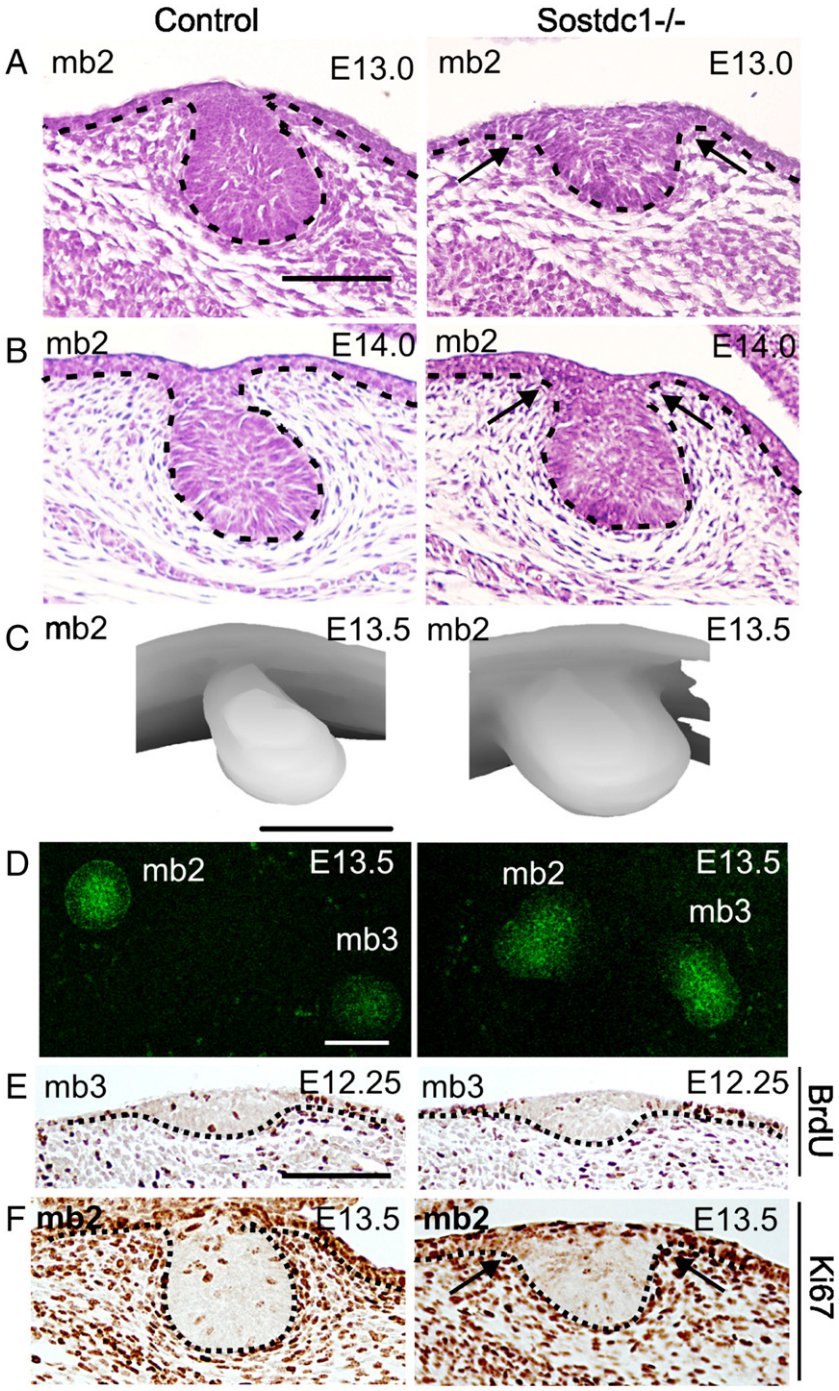

Fig. 3. *Sostdc1*-null mammary buds have enlarged neck region. (A, B) Hematoxylin–eosin stained transverse sections of E13.0 control and *Sostdc1*-null mammary buds (mb) 2. *Sostdc1*-null buds displayed enlarged neck region (arrows), a feature that still persists at E14.0 although the difference was less pronounced. Broken line indicates the border between epithelium and mesenchyme. (C) 3D reconstructions of the serial sections revealed the increased size and enlarged neck of mutant buds whereas the control buds had the characteristic light bulb shape. (D) Confocal images of whole-mount stained mammary buds 2 and 3 with an antibody specific to the epithelial marker EpCAM. (E) In E12.25 mammary bud 3, BrdU incorporation and (F) in E13.5 mammary bud 3, the number of Ki67-positive cells were similar in control and *Sostdc1*-null mice. Scale bars 100 μm.

Wessells, 1984). The most posterior (caudal) and ventral vibrissa placode develops first at E11.0–E11.5, and in general, induction of vibrissae progresses in a posterior to anterior and ventral to dorsal direction. As a result, by E14.5 the final adult pattern of five horizontal rows with one vertical row posterior to them is apparent (Wrenn and Wessells, 1984; see Fig. 6A for vibrissa nomenclature). In addition to primary vibrissae a number of other sensory hairs (secondary vibrissae) develop in the facial region (Fig. 6A). Development of vibrissae proceeded normally in *Sostdc1*-null embryos until E13.0 (data not shown). Interestingly, analysis of *Lef1* and TOP-gal expression revealed ectopic vibrissa placodes at E13.5. These were observed between vibrissa rows 3 and 4, as well as above row 5 (Fig. 6B; Fig. S7). In addition, one ectopic bud was found posterior to the vertical row, next to the Δ follicle, and three to four postoral vibrissa buds developed in all *Sostdc1*-mutants in contrast to two seen in control embryos (Fig. 6B). By E14.5, several supernumerary hair/vibrissa buds were detected throughout the snout (Fig. 6C, D). Accordingly, ectopic mystacial vibrissae, and numerous supernumerary small hair shafts were observed in adult *Sostdc1*-null mice in corresponding positions (Fig. 6E, F).

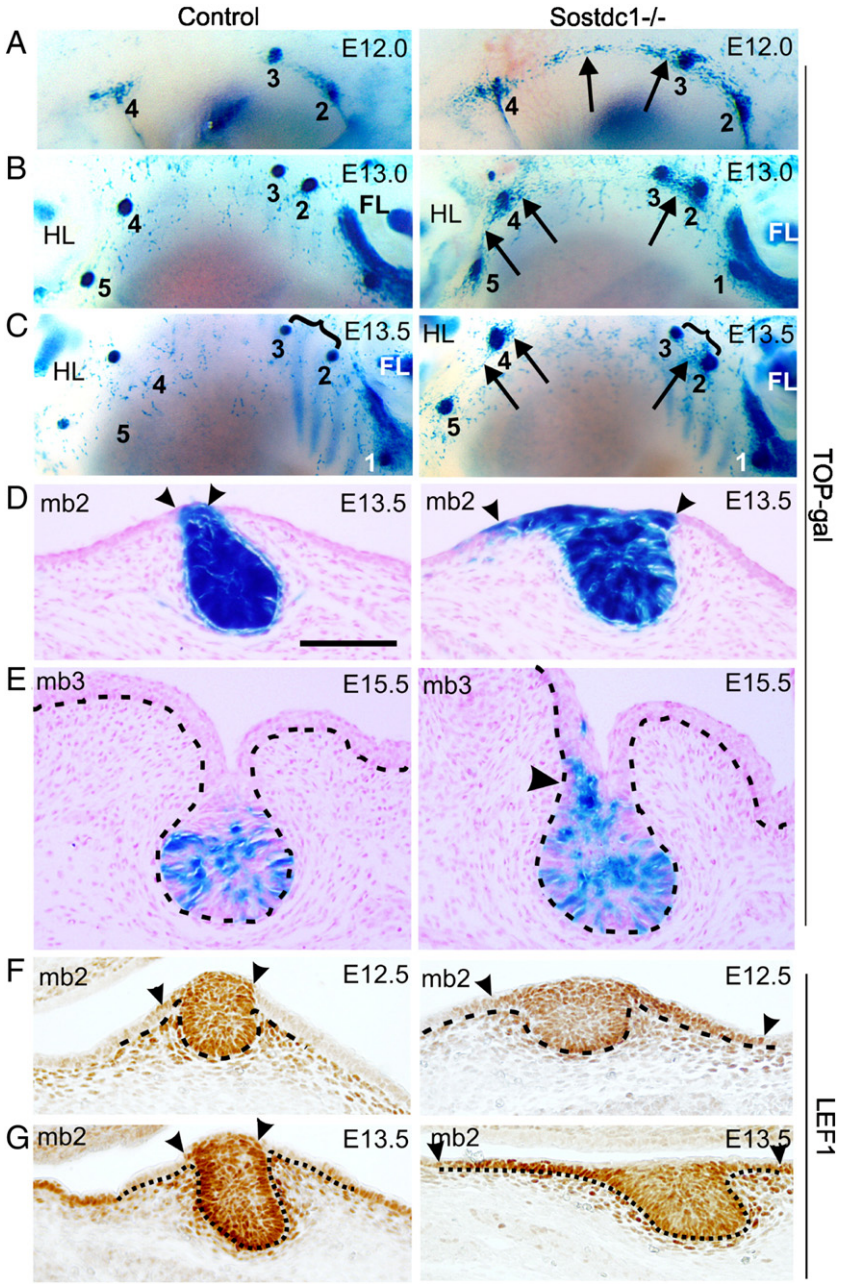

Fig. 4. *Sostdc1*-null mammary buds showed ectopic Wnt activity and LEF1 expression. (A–C) TOPgal expression in E12.0 (A), E13.0 (B), and E13.5 (C) control and *Sostdc1*-null mice. Wnt activity was detected in a larger area in and around *Sostdc1*-null mammary buds (mb) 2–5. Arrows point to TOP-gal-positive cells in milk line between buds 3 and 4 (A), between neighboring mutant buds 2 and 3, and 4 and 5, and next to mammary buds (B, C). Brackets highlight the closer distance between *Sostdc1* −/− mammary buds 2 and 3 compared to control mice (C). (D, E) Transverse sections of X-gal stained TOP-gal mammary buds. The enlarged neck region with ectopic Wnt activity (arrowhead) was evident in *Sostdc1* −/− embryos at E13.5 (D). At E15.5, the bud morphology was similar between control and mutant mice but ectopic Wnt activity (arrowhead) was still observed in the neck region of *Sostdc1* −/− buds (E). (F, G) Immunohistochemical detection of Lef1 in E12.5 (F) and E13.5 (G) mammary buds showed similar LEF1 expression intensity in control and *Sostdc1*-null mammary epithelium and mesenchyme. Broad ectopic LEF1 expression in the epithelial flanks of buds was observed in E12.5 and E13.5 *Sostdc1*-null mice. Arrowheads define the region of the TOP-gal and LEF1 expression in the distal part of mammary bud. Broken lines indicate epithelium–mesenchyme border. Scale bar 100 μm. FL, fore limb; HL, hindlimb.

In order to better visualize vibrissa development, we crossed *Sostdc1*-null mice with K17-GFP transgenic mice expressing GFP under the promoter of keratin 17 (K17) (Bianchi et al., 2005), which is one of the earliest markers associated with placodes in developing skin appendages (McGowan and Coulombe, 1998). *Sostdc1* −/− and control vibrissa pads (Fig. 7A, B) and mandibular skin (Fig. S8) were dissected and cultured in vitro which allowed their continuous monitoring. These data confirmed that a short ectopic vibrissa row formed consistently between rows 3 and 4, placodes appearing in a posterior to anterior direction as in endogenous rows (Fig. 7A, B). Numerous supernumerary vibrissa/hair buds were readily detectable in other locations, as well (Fig. 7A, B; Fig. S8B).

Sostdc1-null mice have enlarged hair primary placodes

Patterning of hair follicles is thought to be established via a reaction–diffusion (R-D) mechanism that operates by secreted molecules that either activate or inhibit follicular fate (Stark et al., 2007). The strong expression of *Sostdc1* around primary hair placodes prompted us to study the size and number of primary hair placodes in *Sostdc1*-

null embryos. Analysis of two placode markers, K17-GFP (Fig. 7C) and *Wnt10b* (Fig. 7D), revealed a slight, yet significant increase in the dimension of primary hair placodes, but not in their number (Fig. 7E; data not shown). In principle, the R-D model could operate with a single activator and its inhibitor that both become focally expressed in nascent hair placodes (or dermal condensates), and the Wnt/Dkk interactions have been proposed to be the key players (Andl et al., 2002; Sick et al., 2006). However, also Eda signaling is involved, at least via its ability to regulate the expression of both Wnts and Dkk4 (Fliniaux et al., 2008; Zhang et al., 2009), as are Bmps which downregulate Edar in interfollicular cells (Mou et al., 2006), but are likely to have also other effects. The fact that *Sostdc1* is not expressed in placodes but around them suggests that Sostdc1 does not act as a typical R-D inhibitor. Rather, Sostdc1 seems to function downstream of Bmps to establish a clear border between Wnt-responsive (placode) and non-responsive (interfollicular cells) and by doing so fine-tunes placode size without affecting their density.

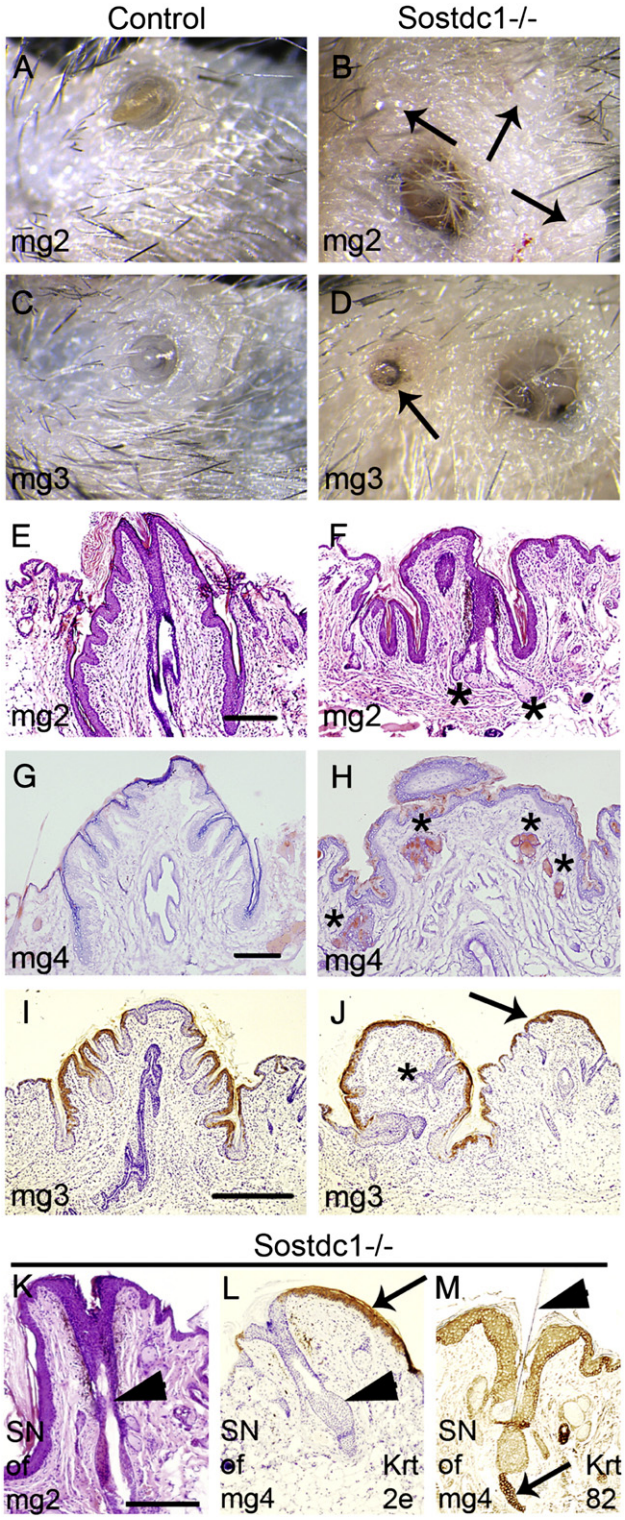

Hair filaments and cycling are not affected by loss of Sostdc1

During advancing stages of hair follicle development, *Sostdc1* transcripts have been detected in the inner root sheath, and the hair bulb (Beaudoin et al., 2005; Laurikkala et al., 2003) suggesting that Sostdc1 could be involved in follicular morphogenesis and/or hair shaft formation. However, the fur and tail hairs of *Sostdc1*-null mice did not differ from those of their littermate controls (Fig. 8A, and data not shown). All hair types (guard, awl, auchene, and zigzag) were found in expected ratios (data not shown), and no abnormalities were detected in the internal structure of hair fibers either (Fig. 8B).

During hair cycle, *Sostdc1* has been detected both in dermal papilla and the follicular epithelium in a dynamic fashion (Beaudoin et al., 2005; O'Shaughnessy et al., 2004). The involvement of Sostdc1 in hair follicle cycling was suggested by studies of *Hairless* (*Hr*) mutant mice (Beaudoin et al., 2005). In *Hr* mice, hair follicles fail to enter the first postnatal anagen (Mann, 1971), and it was proposed that HR could regulate anagen onset by promoting Wnt signaling via repression of *Sostdc1* expression (Beaudoin et al., 2005). We examined hair follicle dynamics during the first highly synchronized hair cycle (Muller-Rover et al., 2001). Between P18 and P20 hair follicles were rapidly regressing in control mice, as they did also in *Sostdc1*-null skin (Fig. 8C–E), and by P21 hair follicles had entered telogen in both genotypes (Fig. 8F). No difference was observed at later stages either (Fig. 8G). Thus, deficiency in *Sostdc1* impedes neither hair fiber production nor hair follicle cycling. Both of these processes are thought to be tightly controlled by Wnt and Bmp signaling (Schneider et al., 2009), and it is possible that loss of *Sostdc1* is compensated by other antagonists of these pathways.

Discussion

Sostdc1 limits the number of vibrissae

Here we have shown that Sostdc1 limits the number of sensory hair and other muzzle hairs. The location and number of murine vibrissa follicles are remarkably constant (Van der Loos et al., 1984; Yamakado and Yohro, 1979). However, the mechanisms governing vibrissa patterning are poorly understood. In outbred ICR mice, supernumerary mystacial vibrissae are not exceptional and rows 5 and 4 may consist of five follicles instead of four (Van der Loos et al., 1984). Interestingly, whenever supernumerary follicles are found

Fig. 5. *Sostdc1*-null mice showed supernumerary nipples and ectopic hair follicles and sebaceous glands in the nipple region. (A–D) Macroscopic views of nipples 2 and 3 in pregnant control and *Sostdc1*−/− mice. Note larger size of mutant nipples. Arrows point to three extra nipple-like structures around the main nipple of mammary gland (mg) 2 and one extra nipple with dark pigment adjacent to mg3. (E, F) The abnormal appearance of Sostdc1−/− nipples was evident in hematoxylin–eosin stained samples. (G, H) Oil Red O staining confirmed the presence of ectopic sebaceous glands in the mutant nipples. (I, J) Expression of the nipple epidermis marker keratin 2e was detected in the endogenous nipples of control and *Sostdc1*−/− mice, as well as in the ectopic nipples (arrow). (K–M) The supernumerary nipples (SN) of *Sostdc1*−/− mg2 (K) and mg4 (L, M) display an ectopic hair follicle (arrowhead in K and L) with orifice in the center of the nipple epidermis. Arrowhead in M indicates a hair filament protruding through the extra nipple. The surface epithelium of ectopic nipples stained positive for keratin 2e (L; arrow), and the hair follicle for keratin82 (M; arrow). Asterisk in F, H, and J points to ectopic pilosebaceous units in the nipples of Sostdc1 mutant mice. Scale bars 200 μm.

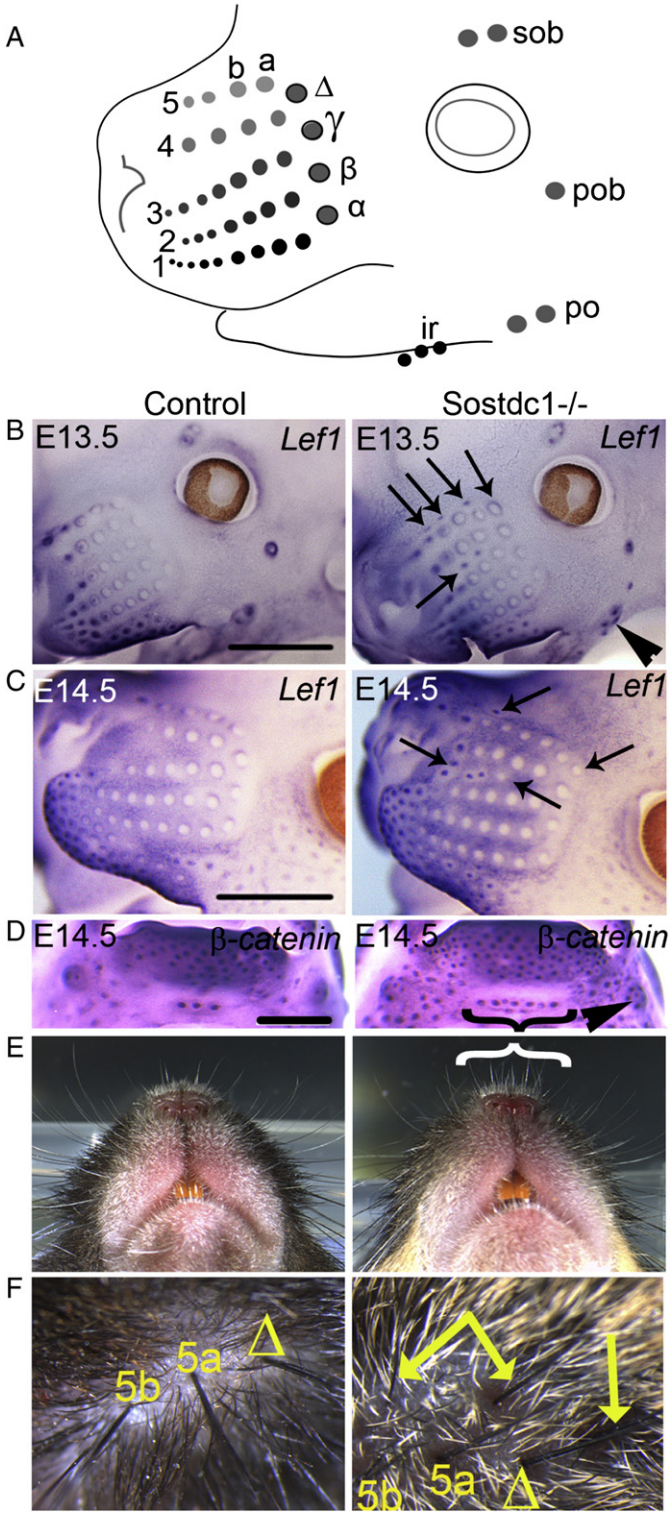

Fig. 6. Supernumerary vibrissae developed in *Sostdc1*-deficient mice. (A) Schematic presentation of the mystacial vibrissa rows (adopted from Wrenn and Wessells, 1984) and supraorbital (sob), postorbital (pob), postoral (po), and inter-ramal (ir) sensory hairs. The five horizontal rows are numbered 1–5. The vibrissae in each row are labeled a, b, … etc. One vertical row comprising Δ, γ, β , and α vibrissae is located posterior to the horizontal rows. (B–D) In *Sostdc1* −/− mice, detection of developing mystacial vibrissae and sensory hairs by *Lef1* and *β-catenin* at E13.5 (B) and E14.5 (C) showed extra vibrissa placodes above row 5, between rows 4 and 3, posterior to Δ , and next to the nostril (arrows). In the mutant mandibular skin, additional postoral (arrowhead) and inter-ramal (bracket) sensory hair placodes were apparent, as well (D). (E) Supernumerary hairs above the nostrils of adult *Sostdc1* −/− mice (bracket). (F) Arrows point to three ectopic whiskers above the endogenous vibrissae Δ, 5a, and 5b in adult *Sostdc1* −/− mice. Scale bars 1 mm.

elsewhere, in ICR or other mouse strains, they are located either above row 5, between rows 3 and 4, or posterior to the horizontal row (Mill et al., 2003; Van der Loos et al., 1984; Yamakado and Yohro, 1979). Notably, a breeding program in ICR mice aiming at maximizing the number of primary vibrissae gave rise to a pattern strikingly similar to that seen in *Sostdc1*-null mice (Van der Loos et al., 1986). These data clearly indicate that supernumerary follicles – when present – develop in non-random positions. The emerging hair placodes are thought to inhibit the neighboring cells from adopting follicular fate (Jiang et al., 2004; Lin et al., 2006; Sick et al., 2006). As the distance between rows 3 and 4 is wider than between other rows (see Fig. 7), it is likely that the inhibitory effect induced by previously formed follicles can be more easily dodged in that location. The same may apply for the other supernumerary follicles that develop at the edges of the vibrissa pad.

We propose that the impact of *Sostdc1* deficiency on vibrissa number is due to increased Wnt/β-cat signaling rather than increased Bmp activity for the following reasons. First, suppression of Bmp activity obtained via overexpression of noggin (i.e. a Bmp pathway manipulation opposite to loss of Sostdc1) causes supernumerary vibrissae to form, although these arise from compound follicles comprising 2–3 vibrissa fibers that share the orifice but have separate lower parts (Plikus et al., 2004). Second, inhibition of canonical Wnt signaling completely blocks initiation of vibrissa development (Andl et al., 2002; Kratochwil et al., 1996) while forced stabilization of epithelial β-catenin (in Catnb$^{\Delta ex3K14/+}$ mice) leads to excessive follicle formation in the whisker pad and e.g. induction of supernumerary postoral vibrissae (Närhi et al., 2008) as also seen in *Sostdc1*-null mice. However, in contrast to Catnb$^{\Delta ex3K14/+}$ embryos, supernumerary vibrissae developed in a rather orderly manner in *Sostdc1*-null mice. Evidently, the spacing of these ectopic placodes is influenced by similar activator–inhibitor cascades regulating the patterning of endogenous vibrissae and pelage hair follicles (Jiang et al., 2004; Mikkola and Millar, 2006). Thus, loss of Sostdc1 allows formation of two ectopic vibrissa rows but other Wnt inhibitors, such as Dkks, sFRPs, or Wif1 are sufficient to ensure regular spacing between individual follicles.

Sostdc1 functions as "a gatekeeper" to limit the number of cells destined to adopt mammary fate

Histology, gene and TOP-gal reporter expression analyses, and whole-mount confocal microscopy revealed the enlarged size and abnormal shape of *Sostdc1*-null mammary primordia. Formation of mammary buds is believed to be the result of cell migration along the mammary line rather than locally enhanced cell proliferation (Balinsky, 1949–50; Propper, 1978; Veltmaat et al., 2003). Earlier studies have shown that between E11.25 and E12.0 a streak of cells expressing mammary placode markers such as *Wnt10b* and TOP-gal extends from mammary placodes towards the neighboring primordia, and it has been proposed that these cells represent migrating cells on their route to the future site of the mammary bud (Chu et al., 2004; Veltmaat et al., 2004). By E12.5, cells expressing placode markers are no longer detected along the mammary line, but are instead almost completely restricted to the definite mammary buds. The fact that in *Sostdc1*-null embryos streaks of placode marker positive cells were observed between the nascent mammary buds even at E13.5 combined with their enlarged size and unaltered cell proliferation does support the cell migration hypothesis as the driving force in mammary bud formation. In this scenario, loss of Sotsdc1 would allow more cells on the mammary line to gain an appendage identity and also enable maintenance of the mammary fate for a longer time leading to an extended period of cell recruitment into the forming buds. Our conclusions are in agreement with a recent cell tracing study which showed that the growth of mammary buds cannot be explained by cell proliferation but is largely driven by an influx of

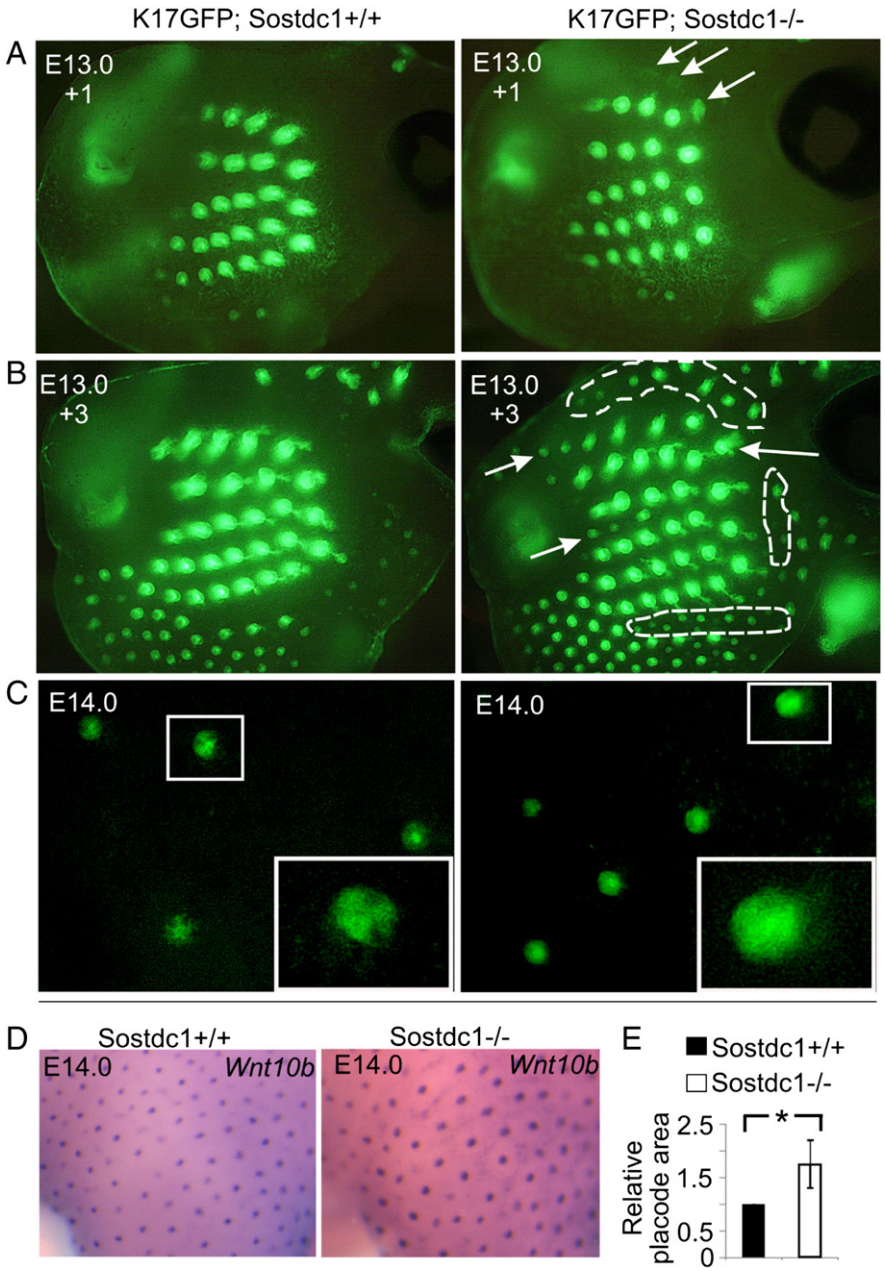

Fig. 7. Monitoring formation of developing mystacial vibrissae and sensory hairs in vitro. (A, B) Vibrissa pads of E13.0 K17-GFP;*Sostdc1*+/+ (n=21) and K17-GFP;*Sostdc1*−/− (n=17) embryos were cultured in vitro for 3 days. Note increasing numbers of mystacial vibrissae (arrows) appearing above row 5 and between rows 3 and 4 in *Sostdc1*−/− specimen. Dashed lines mark areas of numerous other supernumerary hair placodes in the snout of *Sostdc1* mutants. (C, D) Visualization of primary hair placodes in control and *Sostdc1*−/− embryos with K17-GFP (C) and *Wnt10b* (D) at E14.0 revealed a slight increase in the placodal size in mutant embryos. (E) Mean placodal area ±s.d. Five to 21 placodes from identical region were analyzed in each embryo (n=7).*P<0.05.

nearby ectodermal cells (Lee et al., 2011). Perhaps enhanced cell recruitment could account for the increased size of *Sostdc1*-null pelage hair placodes, as well. More detailed studies will be required to confirm these hypotheses.

In principle, Sostdc1 could regulate mammary bud formation either through modulation of the Wnt/β-cat or Bmp pathway, or both. Based on in vitro studies it has been proposed that Bmp4 regulates expression of *Lef1* in the mammary line (Cho et al., 2006), and therefore increased Bmp activity could lead to enhanced Wnt signaling. However, in *Sostdc1*-null embryos ectopic Lef1 mRNA and protein expression correlated with increased TOP-gal and BAT-gal staining, while no changes were observed in pSMAD1/5/8 staining. Therefore, we find it likely that Sostdc1's functions are executed through the canonical Wnt pathway. This conclusion is in line with earlier in vitro studies showing that Wnt pathway stimulation results in formation of enlarged mammary primordia (Chu et al., 2004). Moreover, loss of Lef1, or Wnt co-receptor Lrp5 or Lrp6, has the opposite effect leading to smaller mammary buds with fewer cells (Boras-Granic et al., 2006; Lindvall et al., 2006; Lindvall et al., 2009; van Genderen et al., 1994). Together, these findings fit the idea that Sostdc1 exerts its function as "a gatekeeper" between and around emerging mammary buds, possibly by restricting Wnt signaling which is essential for placodal fate specification.

Sostdc1-null mice display supernumerary nipples and nipple-associated pilosebaceous units

Intriguingly, the absence of *Sostdc1* caused formation of supernumerary rudimentary nipples. In humans, the presence of accessory breast tissue is a rather common phenomenon (Kajava, 1915;

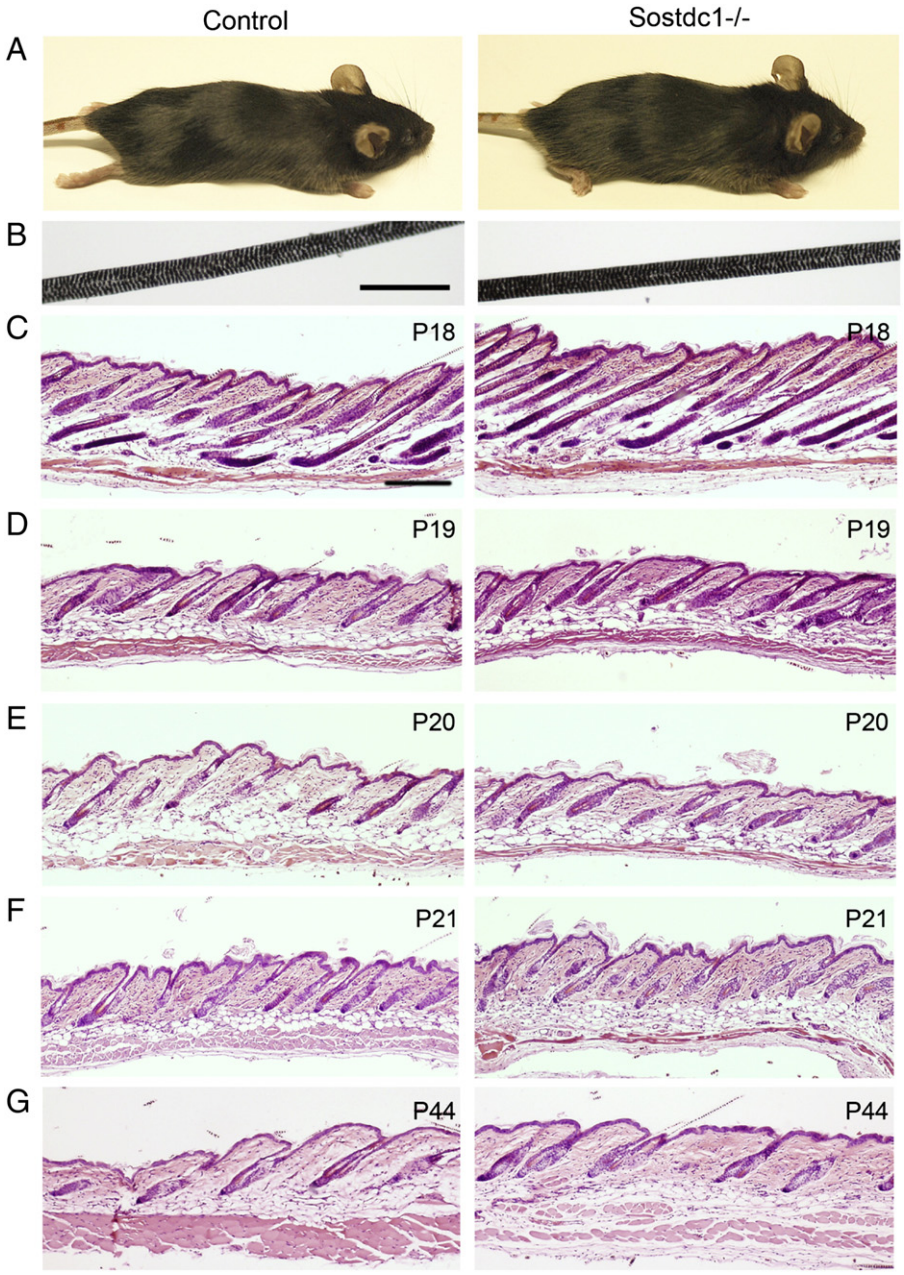

Fig. 8. Hair cycling was unaffected in *Sostdc1* −/− mice. (A) Gross appearance of the pelage of *Sostdc1*-null mice did not differ from control mice. (B) Light microscopic picture of the internal structure of control and Sostdc1 −/− awl hair filament showed three columns of medullary air cells. (C–G) Hematoxylin–eosin stained sections of control and *Sostdc1* −/− dorsal skin from corresponding regions. Progression of the first hair cycle was similar in control and *Sostdc1* −/− mice (C, D) and by P21 (F) hair follicles had entered telogen. At P44 (G), the control and mutant hair follicles were in the second late catagen/telogen stage. Scale bars 200 μm.

Loukas et al., 2007; Velanovich, 1995). It may manifest as supernumerary nipples (polythelia) or less frequently as ectopic breast (polymastia). Supernumerary nipples are almost exclusively located along the milk line, typically just below the normal breast or in the lower axilla, but intra-areolar polythelia has been described as well. Polythelia usually occurs as a sporadic phenomenon, but may also run in families either as a solitary trait or in association with other defects such as kidney abnormalities (Ferrara et al., 2009; Loukas et al., 2007; Velanovich, 1995). The etiology of polythelia is unknown, with the exception of Simpson–Golabi–Behmel syndrome caused by mutations in glypican 3 (DeBaun et al., 2001). It is tempting to speculate that some other types of polythelia could be related with reduced Sostdc1 activity.

In mice, extra nipples are known to develop as a result of Eda overexpression (Mustonen et al., 2003) or alterations in Neuregulin3 expression levels (Howard et al., 2005; Panchal et al., 2007). However, in these cases the nipples and the associated mammary ductal tree arise from ectopic mammary placodes forming in the milk line region (Mustonen et al., 2004; Panchal et al., 2007). The time of induction of ectopic nipples in *Sostdc1*-mutant mice, however, remains elusive, as they were not associated with supernumerary placodes or glandular tissue, and the first morphological features of the embryonic nipple sheaths showed no obvious abnormalities in size or shape (data not shown). Instead, accessory nipples were readily observed only after the onset of puberty when sex steroids are known to increase nipple size indicating that loss of Sostdc1 sensitizes the nipple area to hormonal effects. Whether this happens already during nipple sheath specification at late embryogenesis, or postnatally, is currently not known.

Nipple sheath is thought to be determined around E16, and by E18 a round zone of specialized epidermis has formed, but the molecular

mechanisms governing these processes are poorly known (Veltmaat et al., 2003). Parathyroid hormone related protein (PTHrP) is considered as a key signaling factor in nipple sheath formation. Its effects are mediated by mesenchymal cells expressing PTHrP receptor. In the absence of PTHrP signaling, the mammary mesenchyme is not properly specified, and it in turn fails to instruct the overlying epidermis to differentiate into nipple sheath. On the other hand, ectodermal overexpression of PTHrP results in conversion of the entire ventral epidermis into nipple-like skin devoid of hair follicles (Foley et al., 2001). The effects of PTHrP are thought to be mediated at least in part by Bmp signaling (Hens et al., 2007). On the other hand, also Wnt pathway has been implicated in nipple development: the nipple sheath of *Lrp6*-null mice is considerably smaller at E18.5 (Lindvall et al., 2009). Thus, loss of Sostcd1 could promote formation of ectopic nipple tissue either by enhancing Bmp or Wnt/β-catenin pathway activity, or both.

Sostdc1 deficiency also allowed formation of aberrant pilosebaceous units in the nipple area. Since a similar phenotype has been observed in K14-noggin mice (Mayer et al., 2008), we find it unlikely that the *Sostdc1*-null phenotype is explained by Sostdc1's ability to inhibit Bmp pathway. Recent studies have suggested that a PTHrP-Bmp-Msx2 axis is involved in suppression of hair follicle fate in developing nipples, as deletion of the Bmp effector gene Msx2 restored follicle formation in ventral skin of K14-PTHrP mice (Hens et al., 2007). However, loss of Msx2 on its own does not convert nipple epidermis into hair-bearing epithelium (Mayer et al., 2008). Thus, it seems that either downregulation of Bmp signal (in K14-noggin mice) or upregulation of Wnt activity (in *Sostdc1*-null mice) may enable ectopic hair formation in the normally hairless nipple region. It has been previously suggested that sebaceous gland and hair follicle differentiation require different levels of epithelial Wnt/β-catenin activity (Lo Celso et al., 2004). A similar mechanism could also account for hair follicle and nipple fate determination such that intermediate levels would be sufficient to drive nipple specification while higher levels would be necessary for hair follicle formation.

Conclusions

Taken together, we have shown that Sostdc1, a multifaceted protein with the potential to modulate both Bmp and Wnt pathways, suppresses vibrissa/hair development and mammary bud formation. Earlier studies have shown that Sostdc1 plays an inhibitory role in tooth bud formation (Kassai et al., 2005; Munne et al., 2009; Murashima-Suginami et al., 2007) implying that Sostdc1 has a more general function in determining skin appendage placode number and size. Previous efforts to clarify whether Sostdc1 acts as Bmp or Wnt antagonist in dental tissues have provided ambiguous answers (Kassai et al., 2005; Munne et al., 2009; Murashima-Suginami et al., 2008). However, more recent studies on compound *Sostdc1* and *Lrp5/6* mutant mice suggested that Sostdc1 regulates tooth morphogenesis through suppression of the Wnt/β-catenin pathway (Ahn et al., 2010). We find it likely that also in the context of vibrissa/hair placode and mammary bud formation Sostdc1 functions as a Wnt antagonist.

Acknowledgments

We thank Raija Savolainen, Merja Mäkinen, and Riikka Santalahti for excellent technical assistance and Otso Häärä for the help with statistical analysis. The K17-GFP mice were kindly provided by Pierre Coulombe (Johns Hopkins Bloomberg School of Public Health, Baltimore, MD). This study was financially supported by the Academy of Finland, the Sigrid Jusélius Foundation, and the Helsinki Graduate School in Biotechnology and Molecular Biology.

Appendix A. Supplementary data

Supplementary data to this article can be found online at doi:10.1016/j.ydbio.2012.01.026.

References

Ahn, Y., Sanderson, B.W., Klein, O.D., Krumlauf, R., 2010. Inhibition of Wnt signaling by wise (sostdc1) and negative feedback from Shh controls tooth number and patterning. Development 137, 3221–3231.
Andl, T., Reddy, S.T., Gaddapara, T., Millar, S.E., 2002. WNT signals are required for the initiation of hair follicle development. Dev. Cell. 2, 643–653.
Balinsky, B.I., 1949–50. On the developmental processes in mammary gland and other epidermal structures. Trans. R. Soc. Edinb. 62, 1–31.
Bazzi, H., Fantauzzo, K.A., Richardson, G.D., Jahoda, C.A., Christiano, A.M., 2007. The Wnt inhibitor, dickkopf 4, is induced by canonical wnt signaling during ectodermal appendage morphogenesis. Dev. Biol. 305, 498–507.
Beaudoin III, G.M., Sisk, J.M., Coulombe, P.A., Thompson, C.C., 2005. Hairless triggers reactivation of hair growth by promoting Wnt signaling. Proc. Natl. Acad. Sci. U. S. A. 102, 14653–14658.
Bianchi, N., Depianto, D., McGowan, K., Gu, C., Coulombe, P.A., 2005. Exploiting the keratin 17 gene promoter to visualize live cells in epithelial appendages of mice. Mol. Cell. Biol. 25, 7249–7259.
Blish, K.R., Wang, W., Willingham, M.C., Du, W., Birse, C.E., Krishnan, S.R., Brown, J.C., Hawkins, G.A., Garvin, A.J., D'Agostino Jr., R.B., Torti, F.M., Torti, S.V., 2008. A human bone morphogenetic protein antagonist is down-regulated in renal cancer. Mol. Biol. Cell 19, 457–464.
Boras-Granic, K., Chang, H., Grosschedl, R., Hamel, P.A., 2006. Lef1 is required for the transition of Wnt signaling from mesenchymal to epithelial cells in the mouse embryonic mammary gland. Dev. Biol. 295, 219–231.
Botchkarev, V.A., Botchkareva, N.V., Roth, W., Nakamura, M., Chen, L.H., Herzog, W., Lindner, G., McMahon, J.A., Peters, C., Lauster, R., McMahon, A.P., Paus, R., 1999. Noggin is a mesenchymally derived stimulator of hair-follicle induction. Nat. Cell Biol. 1, 158–164.
Cho, K.W., Kim, J.Y., Song, S.J., Farrell, E., Eblaghie, M.C., Kim, H.J., Tickle, C., Jung, H.S., 2006. Molecular interactions between Tbx3 and Bmp4 and a model for dorsoventral positioning of mammary gland development. Proc. Natl. Acad. Sci. U. S. A. 193, 16788–16793.
Chu, E.Y., Hens, J., Andl, T., Kairo, A., Yamaguchi, T.P., Brisken, C., Glick, A., Wysolmerski, J.J., Millar, S.E., 2004. Canonical WNT signaling promotes mammary placode development and is essential for initiation of mammary gland morphogenesis. Development 131, 4819–4829.
DasGupta, R., Fuchs, E., 1999. Multiple roles for activated lef/tcf transcription complexes during hair follicle development and differentiation. Development 126, 4557–4568.
Davidson, P., Hardy, M.H., 1952. The development of mouse vibrissae in vivo and in vitro. J. Anat. 86, 342–356.
DeBaun, M.R., Ess, J., Saunders, S., 2001. Simpson Golabi Behmel syndrome: progress toward understanding the molecular basis for overgrowth, malformation, and cancer predisposition. Mol. Genet. Metab. 72, 279–286.
Ferrara, P., Giorgio, V., Vitelli, O., Gatto, A., Romano, V., Bufalo, F.D., Nicoletti, A., 2009. Polythelia: still a marker of urinary tract anomalies in children? Scand. J. Urol. Nephrol. 43, 47–50.
Fliniaux, I., Mikkola, M.L., Lefebvre, S., Thesleff, I., 2008. Identification of dkk4 as a target of Eda-A1/Edar pathway reveals an unexpected role of ectodysplasin as inhibitor of wnt signalling in ectodermal placodes. Dev. Biol. 320, 60–71.
Foley, J., Dann, P., Hong, J., Cosgrove, J., Dreyer, B., Rimm, D., Dunbar, M., Philbrick, W., Wysolmerski, J., 2001. Parathyroid hormone-related protein maintains mammary epithelial fate and triggers nipple skin differentiation during embryonic breast development. Development 128, 513–525.
Harris, M.P., Linkhart, B.L., Fallon, J.F., 2004. Bmp7 mediates early signaling events during induction of chick epidermal organs. Dev. Dyn. 231, 22–32.
Hens, J.R., Dann, P., Zhang, J.P., Harris, S., Robinson, G.W., Wysolmerski, J., 2007. BMP4 and PTHrP interact to stimulate ductal outgrowth during embryonic mammary development and to inhibit hair follicle induction. Development 134, 1221–1230.
Hollnagel, A., Oehlmann, V., Heymer, J., Ruther, U., Nordheim, A., 1999. Id genes are direct targets of bone morphogenetic protein induction in embryonic stem cells. J. Biol. Chem. 274, 19838–19845.
Howard, B., Panchal, H., McCarthy, A., Ashworth, A., 2005. Identification of the scaramanga gene implicates neuregulin3 in mammary gland specification. Genes Dev. 19, 2078–2090.
Itasaki, N., Jones, C.M., Mercurio, S., Rowe, A., Domingos, P.M., Smith, J.C., Krumlauf, R., 2003. Wise, a context-dependent activator and inhibitor of Wnt signalling. Development 130, 4295–4305.
Järvinen, E., Salazar-Ciudad, I., Birchmeier, W., Taketo, M.M., Jernvall, J., Thesleff, I., 2006. Continuous tooth generation in mouse is induced by activated epithelial Wnt/beta-catenin signaling. Proc. Natl. Acad. Sci. U. S. A. 103, 18627–18632.
Järvinen, E., Tummers, M., Thesleff, I., 2009. The role of the dental lamina in mammalian tooth replacement. J. Exp. Zool. B Mol. Dev. Evol. 312B, 281–291.
Jiang, T.X., Widelitz, R.B., Shen, W.M., Will, P., Wu, D.Y., Lin, C.M., Jung, H.S., Chuong, C.M., 2004. Integument pattern formation involves genetic and epigenetic controls: feather arrays simulated by digital hormone models. Int. J. Dev. Biol. 48, 117–135.

Jung, H.S., Francis-West, P.H., Widelitz, R.B., Jiang, T.X., Ting-Berreth, S., Tickle, C., Wolpert, L., Chuong, C.M., 1998. Local inhibitory action of BMPs and their relationships with activators in feather formation: implications for periodic patterning. Dev. Biol. 196, 11–23.

Kajava, Y., 1915. Yliluku isten nisien esiintymisestä suomalaisilla (in Finnish). Duodecim 31, 143–170.

Kassai, Y., Munne, P., Hotta, Y., Penttila, E., Kavanagh, K., Ohbayashi, N., Takada, S., Thesleff, I., Jernvall, J., Itoh, N., 2005. Regulation of mammalian tooth cusp patterning by ectodin. Science 309, 2067–2070.

Kiyozumi, D., Osada, A., Sugimoto, N., Weber, C.N., Ono, Y., Imai, T., Okada, A., Sekiguchi, K., 2010. Identification of genes expressed during hair follicle induction. J. Dermatol. 38, 674–679.

Kratochwil, K., Dull, M., Farinas, I., Galceran, J., Grosschedl, R., 1996. Lef1 expression is activated by BMP-4 and regulates inductive tissue interactions in tooth and hair development. Genes Dev. 10, 1382–1394.

Lane, T.F., Leder, P., 1997. Wnt-10b directs hypermorphic development and transformation in mammary glands of male and female mice. Oncogene 15, 2133–2144.

Laurikkala, J., Pispa, J., Jung, H.S., Nieminen, P., Mikkola, M., Wang, X., Saarialho-Kere, U., Galceran, J., Grosschedl, R., Thesleff, I., 2002. Regulation of hair follicle development by the TNF signal ectodysplasin and its receptor Edar. Development 129, 2541–2553.

Laurikkala, J., Kassai, Y., Pakkasjarvi, L., Thesleff, I., Itoh, N., 2003. Identification of a secreted BMP antagonist, ectodin, integrating BMP, FGF, and SHH signals from the tooth enamel knot. Dev. Biol. 264, 91–105.

Lee, M.Y., Racine, V., Jagadpramana, P., Sun, L., Yu, W., Du, T., Spencer-Dene, B., Rubin, N., Le, L., Ndiaye, D., Bellusci, S., Kratochwil, K., Veltmaat, J.M., 2011. Ectodermal influx and cell hypertrophy provide early growth for all murine mammary rudiments, and are differentially regulated among them by Gli3. PLoS One 6, e26242.

Leimeister, C., Bach, A., Gessler, M., 1998. Developmental expression patterns of mouse sFRP genes encoding members of the secreted frizzled related protein family. Mech. Dev. 75, 29–42.

Lin, C.M., Jiang, T.X., Widelitz, R.B., Chuong, C.M., 2006. Molecular signaling in feather morphogenesis. Curr. Opin. Cell Biol. 18, 730–741.

Lindvall, C., Evans, N.C., Zylstra, C.R., Li, Y., Alexander, C.M., Williams, B.O., 2006. The Wnt signaling receptor Lrp5 is required for mammary ductal stem cell activity and Wnt1-induced tumorigenesis. J. Biol. Chem. 281, 35081–35087.

Lindvall, C., Zylstra, C.R., Evans, N., West, R.A., Dykema, K., Furge, K.A., Williams, B.O., 2009. The Wnt co-receptor Lrp6 is required for normal mouse mammary gland development. PLoS One 4, e5813.

Lintern, K.B., Guidato, S., Rowe, A., Saldanha, J.W., Itasaki, N., 2009. Characterization of wise protein and its molecular mechanism to interact with both Wnt and BMP signals. J. Biol. Chem. 284, 23159–23168.

Lo Celso, C., Prowse, D.M., Watt, F.M., 2004. Transient activation of beta-catenin signalling in adult mouse epidermis is sufficient to induce new hair follicles but continuous activation is required to maintain hair follicle tumours. Development 131, 1787–1799.

Loukas, M., Clarke, P., Tubbs, R.S., 2007. Accessory breasts: a historical and current perspective. Am. Surg. 73, 525–528.

Mahler, B., Gocken, T., Brojan, M., Childress, S., Spandau, D.F., Foley, J., 2004. Keratin 2e: a marker for murine nipple epidermis. Cells Tissues Organs 176, 169–177.

Mann, S.J., 1971. Hair loss and cyst formation in hairless and rhino mutant mice. Anat. Rec. 170, 485–499.

Maretto, S., Cordenonsi, M., Dupont, S., Braghetta, P., Broccoli, V., Hassan, A.B., Volpin, D., Bressan, G.M., Piccolo, S., 2003. Mapping Wnt/beta-catenin signaling during mouse development and in colorectal tumors. Proc. Natl. Acad. Sci. U. S. A. 100, 3299–3304.

Mayer, J.A., Foley, J., De La Cruz, D., Chuong, C.M., Widelitz, R., 2008. Conversion of the nipple to hair-bearing epithelia by lowering bone morphogenetic protein pathway activity at the dermal–epidermal interface. Am. J. Pathol. 173, 1339–1348.

McGowan, K.M., Coulombe, P.A., 1998. Onset of keratin 17 expression coincides with the definition of major epithelial lineages during skin development. J. Cell Biol. 143 (2), 469–486 19.

Michon, F., Forest, L., Collomb, E., Demongeot, J., Dhouailly, D., 2008. BMP2 and BMP7 play antagonistic roles in feather induction. Development 135, 2797–2805.

Mikkola, M.L., 2007. Genetic basis of skin appendage development. Semin. Cell Dev. Biol. 18, 225–236.

Mikkola, M.L., Millar, S.E., 2006. The mammary bud as a skin appendage: unique and shared aspects of development. J. Mammary Gland Biol. Neoplasia 11, 187–203.

Mill, P., Mo, R., Fu, H., Grachtchouk, M., Kim, P.C., Dlugosz, A.A., Hui, C.C., 2003. Sonic hedgehog-dependent activation of Gli2 is essential for embryonic hair follicle development. Genes Dev. 17, 282–294.

Mou, C., Jackson, B., Schneider, P., Overbeek, P.A., Headon, D.J., 2006. Generation of the primary hair follicle pattern. Proc. Natl. Acad. Sci. U. S. A. 103, 9075–9080.

Muller-Rover, S., Handjiski, B., van der Veen, C., Eichmuller, S., Foitzik, K., McKay, I.A., Stenn, K.S., Paus, R., 2001. A comprehensive guide for the accurate classification of murine hair follicles in distinct hair cycle stages. J. Invest. Dermatol. 117, 3–15.

Munne, P.M., Tummers, M., Jarvinen, E., Thesleff, I., Jernvall, J., 2009. Tinkering with the inductive mesenchyme: sostdc1 uncovers the role of dental mesenchyme in limiting tooth induction. Development 136, 393–402.

Murashima-Suginami, A., Takahashi, K., Kawabata, T., Sakata, T., Tsukamoto, H., Sugai, M., Yanagita, M., Shimizu, A., Sakurai, T., Slavkin, H.C., Bessho, K., 2007. Rudiment incisors survive and erupt as supernumerary teeth as a result of USAG-1 abrogation. Biochem. Biophys. Res. Commun. 359, 549–555.

Murashima-Suginami, A., Takahashi, K., Sakata, T., Tsukamoto, H., Sugai, M., Yanagita, M., Shimizu, A., Sakurai, T., Slavkin, H.C., Bessho, K., 2008. Enhanced BMP signaling results in supernumerary tooth formation in USAG-1 deficient mouse. Biochem. Biophys. Res. Commun. 369, 1012–1016.

Mustonen, T., Pispa, J., Mikkola, M.L., Pummila, M., Kangas, A.T., Pakkasjarvi, L., Jaatinen, R., Thesleff, I., 2003. Stimulation of ectodermal organ development by ectodysplasin-A1. Dev. Biol. 259, 123–136.

Mustonen, T., Ilmonen, M., Pummila, M., Kangas, A.T., Laurikkala, J., Jaatinen, R., Pispa, J., Gaide, O., Schneider, P., Thesleff, I., Mikkola, M.L., 2004. Ectodysplasin A1 promotes placodal cell fate during early morphogenesis of ectodermal appendages. Development 131, 4907–4919.

Närhi, K., Thesleff, I., 2010. Explant culture of embryonic craniofacial tissues: analyzing effects of signaling molecules on gene expression. Methods Mol. Biol. 666, 253–267.

Närhi, K., Jarvinen, E., Birchmeier, W., Taketo, M.M., Mikkola, M.L., Thesleff, I., 2008. Sustained epithelial beta-catenin activity induces precocious hair development but disrupts hair follicle down-growth and hair shaft formation. Development 135, 1019–1028.

Noramly, S., Morgan, B.A., 1998. BMPs mediate lateral inhibition at successive stages in feather tract development. Development 125, 3775–3787.

O'Shaughnessy, R.F., Yeo, W., Gautier, J., Jahoda, C.A., Christiano, A.M., 2004. The WNT signalling modulator, wise, is expressed in an interaction-dependent manner during hair-follicle cycling. J. Invest. Dermatol. 123, 613–621.

Panchal, H., Wansbury, O., Parry, S., Ashworth, A., Howard, B., 2007. Neuregulin3 alters cell fate in the epidermis and mammary gland. BMC Dev. Biol. 7, 105.

Plikus, M., Wang, W.P., Liu, J., Wang, X., Jiang, T.X., Chuong, C.M., 2004. Morpho-regulation of ectodermal organs: integument pathology and phenotypic variations in K14-Noggin engineered mice through modulation of bone morphogenic protein pathway. Am. J. Pathol. 164, 1099–1114.

Propper, A.Y., 1978. Wandering epithelial cells in the rabbit embryo milk line. A preliminary scanning electron microscope study. Dev. Biol. 67, 225–231.

Pummila, M., Fliniaux, I., Jaatinen, R., James, M.J., Laurikkala, J., Schneider, P., Thesleff, I., Mikkola, M.L., 2007. Ectodysplasin has a dual role in ectodermal organogenesis: inhibition of Bmp activity and induction of Shh expression. Development 134, 117–125.

Rice, D.P., Aberg, T., Chan, Y., Tang, Z., Kettunen, P.J., Pakarinen, L., Maxson, R.E., Thesleff, I., 2000. Integration of FGF and TWIST in calvarial bone and suture development. Development 127, 1845–1855.

Schneider, M.R., Schmidt-Ullrich, R., Paus, R., 2009. The hair follicle as a dynamic miniorgan. Curr. Biol. 19, R132–R142.

Sick, S., Reinker, S., Timmer, J., Schlake, T., 2006. WNT and DKK determine hair follicle spacing through a reaction–diffusion mechanism. Science 314, 1447–1450.

Simmons, D.G., Kennedy, T.G., 2002. Uterine sensitization-associated gene-1: a novel gene induced within the rat endometrium at the time of uterine receptivity/sensitization for the decidual cell reaction. Biol. Reprod. 67, 1638–1645.

Stark, J., Andl, T., Millar, S.E., 2007. Hairy math: insights into hair-follicle spacing and orientation. Dev. Cell 128, 17–20.

Tsukamoto, A.S., Grosschedl, R., Guzman, R.C., Parslow, T., Varmus, H.E., 1988. Expression of the int-1 gene in transgenic mice is associated with mammary gland hyperplasia and adenocarcinomas in male and female mice. Cell 55, 619–625.

Tummers, M., Thesleff, I., 2009. The importance of signal pathway modulation in all aspects of tooth development. J. Exp. Zool. B Mol. Dev. Evol. 312B, 309–319.

Van der Loos, H., Dorfl, J., Welker, E., 1984. Variation in pattern of mystacial vibrissae in mice. a quantitative study of ICR stock and several inbred strains. J. Hered. 75, 326–336.

Van der Loos, H., Welker, E., Dorfl, J., Rumo, G., 1986. Selective breeding for variations in patterns of mystacial vibrissae of mice. Bilaterally symmetrical strains derived from icr stock. J. Hered. 77, 66–82.

van Genderen, C., Okamura, R.M., Farinas, I., Quo, R.G., Parslow, T.G., Bruhn, L., Grosschedl, R., 1994. Development of several organs that require inductive epithelial–mesenchymal interactions is impaired in LEF-1-deficient mice. Genes Dev. 8, 2691–2703.

Velanovich, V., 1995. Ectopic breast tissue, supernumerary breasts, and supernumerary nipples. South. Med. J. 88, 903–906.

Veltmaat, J.M., Mailleux, A.A., Thiery, J.P., Bellusci, S., 2003. Mouse embryonic mammogenesis as a model for the molecular regulation of pattern formation. Differentiation 71, 1–17.

Veltmaat, J.M., Van Veelen, W., Thiery, J.P., Bellusci, S., 2004. Identification of the mammary line in mouse by Wnt10b expression. Dev. Dyn. 229, 349–356.

Wang, J., Shackleford, G.M., 1996. Murine Wnt10a and Wnt10b: cloning and expression in developing limbs, face and skin of embryos and in adults. Oncogene 13, 1537–1544.

Wrenn, J.T., Wessells, N.K., 1984. The early development of mystacial vibrissae in the mouse. J. Embryol. Exp. Morphol. 83, 137–156.

Yamakado, M., Yohro, T., 1979. Subdivision of mouse vibrissae on an embryological basis, with descriptions of variations in the number and arrangement of sinus hairs and cortical barrels in BALB/c (Nu/+; Nude, nu/nu) and hairless (hr/hr) strains. Am. J. Anat. 155, 153–173.

Yanagita, M., Oka, M., Watabe, T., Iguchi, H., Niida, A., Takahashi, S., Akiyama, T., Miyazono, K., Yanagisawa, M., Sakurai, T., 2004. USAG-1: a bone morphogenetic protein antagonist abundantly expressed in the kidney. Biochem. Biophys. Res. Commun. 316, 490–500.

Zhang, Y., Tomann, P., Andl, T., Gallant, N.M., Huelsken, J., Jerchow, B., Birchmeier, W., Paus, R., Piccolo, S., Mikkola, M.L., Morrisey, E.E., Overbeek, P.A., Scheidereit, C., Millar, S.E., Schmidt-Ullrich, R., 2009. Reciprocal requirements for EDA/EDAR/NF-kappaB and Wnt/beta-catenin signaling pathways in hair follicle induction. Dev. Cell 17, 49–61.

Zhang, J., Li, Y., Liu, Q., Lu, W., Bu, G., 2010. Wnt signaling activation and mammary gland hyperplasia in MMTV-LRP6 transgenic mice: implication for breast cancer tumorigenesis. Oncogene 29, 539–549.